MODE DECOMPOSITION OF A TAPERED FREE ELECTRON LASER

S.D. Chen, K. Fang, X. Huang, C. Pellegrini, J. Wu, SLAC, CA 94025, USA
K. Fang, Indiana University, IN 47405, USA
C. Emma, C. Pellegrini, University of California, Los Angeles, CA 90095, USA
S.D. Chen, C.S. Hwang, NCTU, Hsinchu 30076, Taiwan
C.S. Hwang, NSRRC, Hsinchu 30076, Taiwan
S. Serkez, Deutsches Elektronen-Synchrotron, 22607 Hamburg, Germany

Abstract

For the ultimate use for the scientific experiments, the free electron laser (FEL) will propagate for long distance, much longer than the Rayleigh range, after exiting the undulator. To characterize the FEL for this purpose, we study the electromagnetic field mode components of the FEL photon beam. With the mode decomposition, the transverse coherence can be analyzed all along. The FEL here in this paper is a highly tapered one evolving through the exponential growth and then the post-saturation taper. Modes contents are analyzed for electron bunch with three different types of transverse distribution: flattop, Gaussian, and parabolic. The tapered FEL simulation is performed with Genesis code. The FEL photon beam transverse electric field is decomposed with Gaussian-Laguerre polynomials. The evolutions of spot size, source location, and the portion of the power in the fundamental mode are discussed here. The approach can be applicable to various kind scheme of FEL.

INTRODUCTION

Free electron Laser (FEL) is one of the most powerful tools for frontier scientific research. Many experiments, especially for bioimaging [1, 2], will benefit greatly from the enhanced coherent light peak power at Terawatt (TW) level. To improve the efficiency of an FEL, in recent years, the tapered undulator scheme has gotten renewed attentions [3–5]. More recently, to further improve the taper efficiency, various transverse distributions of the electron bunch are investigated. In this paper, we study this topic by looking into the mode contents of the FEL in the exponential growth regime as well as in the post-saturation tapered regime.

As initiated in Ref. [5], the transverse effect is also an important aspect to be studied for boosting the FEL power into TW level. In this paper, three different types of transverse distributions of the electron beam, the flattop, Gaussian, and parabolic distributions, are analyzed. Different transverse distributions can excite different kinds of high-order modes, which can in principle help trapping the electrons as the FEL interaction develops along the undulator field. Therefore, the FEL power can be further increased. With the mode contents analyzed, the transverse coherence can be studied naturally. The mode decomposition, which is to decompose a field to a set of complete orthonormal modes, is widely used on laser like high directional sources [6].

To compare with the decomposition method, a simple analytical extended "line source" model is developed. The decomposition result and the evolution of the spot size, the source location and the power ratio of fundamental mode to the total power are presented.

LAGUERRE-GAUSSIAN EXPANSION

A complex E-field with the form of $\tilde{E}(x,y)$ can be expanded in a complete orthnormal basis. Here the Laguerre-Gaussian polynomials are chosen as the basis for expansion:

$$E(r) = \sum_{n=0}^{\infty} a_n e^{-\zeta r^2/2} L_n\left(\Re(\zeta) r^2\right), \qquad (1)$$

where we assume that the modes have azimuthal symmetry $r = \sqrt{x^2 + y^2}$ with $\Re(\zeta)$ being the real part of ζ which characterizes the mode size and also the wave-front curvature. With the orthogonality condition, the coefficients a_n can be calculated, and the square of a_n fives the power of each mode.

We get the electric field as a numerical solution from GENESIS [7] simulation. The electric field output is a two-dimensional matrix with complex values, which is in the form of $\tilde{E}(\Delta x m_1, \Delta y m_2)$, where m_1 and m_2 are integers. The a_n should be integrated by discretized form of

$$a_n = \sum_{m_1} \sum_{m_2} \tilde{E}(\Delta x m_1, \Delta y m_2) \exp\left(\frac{-\zeta}{2} r^2\right) * L_n\left(\Re(\zeta) r^2\right) \Re(\zeta) \Delta x \Delta y, \qquad (2)$$

where r^2should be substituted by $(\Delta x m_1)^2 + (\Delta y m_2)^2$.

We have carefully chosen the grid size and simulation area such that the orthogonality between different Laguerre-Gaussian modes is well preserved. The grid size is small enough to represent the structure in Laguerre-Gaussian modes, while the simulation area is large enough so that the cutoff error is negligible.

Based on the above formalism, an electric field can be decomposed numerically by the mode series of a Laguerre-Gaussian polynomial. However, the set of mode series are not determined until the value ζ is fixed. Although conceptually the basis is complete for an arbitrary complex value of ζ, physics consideration has to be applied to find ζ. The details of our approach is given in next section.

ISBN 978-3-95450-133-5

DECOMPOSITION METHOD

The electric field expression in Eq. (1) is analogous to a standard Gaussian laser beam. For $n = 0$ in Eq. (1), at a certain z, we can have the relations:

$$\Re(\zeta) = \frac{2}{w^2(z)}, \quad (3)$$

and

$$\Im(\zeta) = \frac{k}{R(z)}, \quad (4)$$

where $\Im(\zeta)$ is the imaginary part of ζ.$R(z)$ and $w(z)$ stands for the wave-front curvature and the spot size, respectively. The above relations clearly expresses the physical and mathematical meaning of ζ, and the relations help us develop a brief approach of finding the value ζ.

Let's discuss the imaginary part of ζ first. For free space propagation of a divergent field $\tilde{E}(\Delta x m_1, \Delta y m_2)$ at z, the rms spot size (σ_r) increases as in the $+z$-direction; and σ_r decreases as in the $-z$-direction (and vice versa for a convergent photon beam). One special case is that σ_r increases in both propagation directions ($\pm z$-directions), when the wave-front curvature is infinity. In other words, writing the electric field in the following form:

$$\tilde{E}(\Delta x m_1, \Delta y m_2) = \tilde{E}_0 e^{-ia} \exp\left[-ibr^2 - cr^2\right], \quad (5)$$

such a special case happens at $b = 0$. Normally, $b = \Im(\zeta) \neq 0$ for an arbitrary z. However, by multiplying a term, $\exp\left[ib'r^2\right]$ to Eq. (5), the propagation property will be changed. If $b' = b$, $\exp\left[ib'r^2\right] \times \tilde{E}(\Delta x m_1, \Delta y m_2)$ has the property of the special case, *i.e.*, σ_r increases in both the $+z$ and the $-z$ directions, then we have b' right equal to $\Im(\zeta)$. This is how we find $\Im(\zeta)$.

Now, let's discuss the real part of ζ. In Ref. [8], a Variational-Solution-Based (VSB) expansion method was adopted to solve the dispersion relation of an FEL system with a trial function in Gaussian form. The solution of the dispersion relation tells us that the fundamental eigenmode [$n = 0$ in Eq. (1)] has the largest growth rate and eventually the fundamental eigenmode dominates the electric field. So a simple rule could be adopted for choosing $\Re(\zeta)$, *i.e.*, the chosen $\zeta = \Re(\zeta) + i\Im(\zeta)$ should maximize the portion of the fundamental mode, while the $\Im(\zeta)$ should be fixed by the propagation approach described above.

Before we explain the details of the mode content, let us give the parameters of the simulation as in Tab. 1. For the particular example in this paper, we are simulating a seeded FEL in a highly tapered undulator and reaches TW level as shown in Fig. 1 for three different electron transverse distributions: Flattop, Gaussian, and Parabolic. Within about 180 meter long undulator, the FEL power can reach TW level for all the three different distributions, with the flattop distribution supporting the highest power. The seed is a Gaussian fundamental mode with 5 MW peak power.

Here is a brief description of the approach:

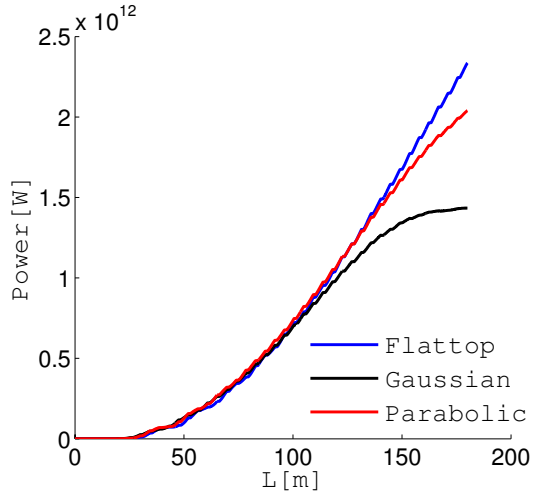

Figure 1: FEL power along the undulator for three different distributions: Flattop, Gaussian, and Parabolic.

Table 1: The Parameters Used in The Simulation in This Paper

Symbol	Value	Unit
Charge Q	150	pC
Centroid energy E_0	13.64	GeV
Peak current I_{pk}	4	kA
Temporal distribution	flattop	-
Slice normalized emittance ε_n	0.3	mm-mrad
Slice energy spread σ_δ	9.5	10^{-5}
Undulator period λ_w	3.2	cm
Length of undulator L_w	180	m
FEL wavelength λ_r	1.5	Å
FEL seed power P_{seed}	5	MW
Power gain length L_G	2.7	m

1. Get $\Im(\zeta)$ by studying the wave front curvature property via free space propagation.

2. Get $\Re(\zeta)$ by maximizing the portion of fundamental mode.

The summation of modes from decomposition calculation is then compared with the electric field from GENESIS output. Results for three typical values of z, namely: in the exponential growth region ($z = 20$ m), at the exponential growth saturation point ($z = 30$ m), and post exponential growth saturation region ($z = 150$ m), are presented in Fig. 2. The results show that the approach works well. Even though the curve inside the central parabolic region of the phase plot (right column in Fig. 2) deviates from a parabolic curve, it still gives a very nice match, which gives a strong proof that a_n calculated by Eq. (2) gives correct amplitude and phase

ISBN 978-3-95450-133-5

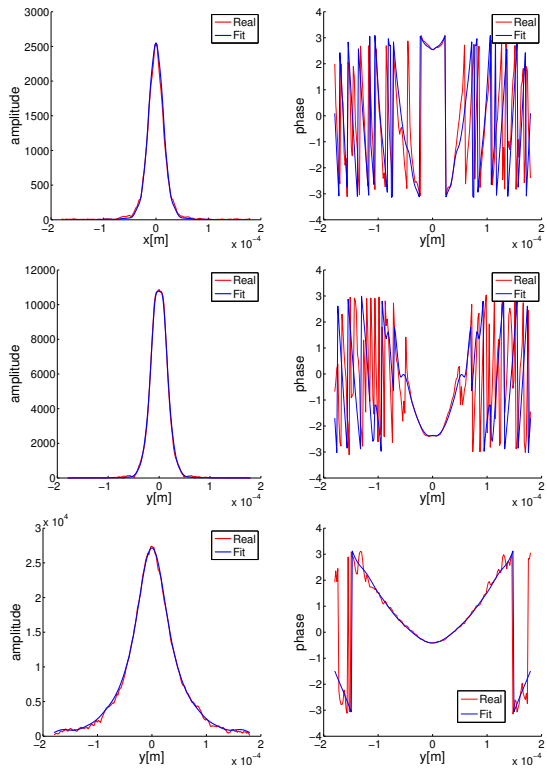

Figure 2: The absolute value and the phase of the $E(r) = \sum_{n=0}^{19} a_n e_{\zeta n}$ (from decomposition calculation) and $\tilde{E}(\Delta x m_1, \Delta y m_2)$ (from the GENESIS simulation) are plotted. Three cases with $z = 20, 30$, and 150 m represent the exponential growth region, the saturation point, and the post saturation region, respectively.

of the modes. According to the results, the electric field data can be well reconstructed with about twenty modes. The discrepancy of the phase in the large r-region is due to the numerical reflection field from the boundary in GENESIS simulation. Furthermore, there is very little FEL power in this large r-region. The evolution of the spot size and the source location is discussed after next section.

THEORETICAL MODEL: A LINE SOURCE

In the post-saturation region after the exponential growth, the FEL photon can be modeled as an extended line source. The light emitted from a long undulator in the post-saturation region is analogous to an extended line source containing infinite points from which a laser beam is emitted at its waist position. The line source points are weighted by the following function,

$$p^{\alpha,\beta}(z_s, z_{\rm sat}) = 1 + \alpha (z_s - z_{\rm sat})^{\beta}, \qquad (6)$$

where z_s is the source location, and $z_{\rm sat}$ is the exponential growth saturation point. The weighting function in Eq. (6) as a physics consideration is to describe the fact that the local emitted power is varying along the undulator. For $\beta = 0$, Eq. (6) describes a scenario that the local emitted power is the same along the undulator, so that the total power will be increasing linearly along the undulator. While for $\beta = 1$, Eq. (6) then describes that the local emitted power is increasing linearly along the undulator, so that the total power will be increasing quadratically along the undulator.

For the case that the observation point z is outside of the undulator, *i.e.* $z > L_u$, an integration from the exponential growth saturation point $z_{\rm sat}$ to the undulator exit L_u then describes how the spot size evolves in such a line source model,

$$w^2(z, L_u) = \frac{\int_{z_{\rm sat}}^{L_u} w_0^2 \left[1 + \left(\frac{z - z_s}{z_R}\right)^2\right] p^{\alpha,\beta}(z_s, z_{\rm sat})\, dz_s}{\int_{z_{\rm sat}}^{L_u} p^{\alpha,\beta}(z_s, z_{\rm sat})\, dz_s}, \qquad (7)$$

where the subscript in z_s means "source" which can be anywhere from the exponential growth saturation point, z_{sat}, to the end of undulator at L_u; $z_R = \pi w_0^2/\lambda_r$ is the Rayleigh range and w_0 is the beam waist size.

Normally, the second term in the weighting function as in Eq. (6) is much larger than the first term: "1", so the first term is dropped in the following calculation for simplicity even though the integral in Eq. (7) can still lead to a closed form with the first term: "1". With the first term dropped, the parameter α is canceled out, so the integral in Eq. (7) becomes:

$$w_\beta^2(z, L_u) = \frac{w_0^2}{z_R^2} \frac{(1+\beta)\Gamma(1+\beta)}{\Gamma(4+\beta)} \times \left[(1+\beta)(3+\beta)(z - L_u)^2 + (3+\beta)(z - z_{\rm sat})^2 - (1+\beta)(L_u - z_{\rm sat})^2 + (2+\beta)(3+\beta) z_R^2\right]. \qquad (8)$$

For $\beta = 0$ and $\beta = 1$, the expressions are:

$$w_{\beta=0}^2(z, L_u) = w_0^2 \left[1 + \frac{(z - L_u)^2}{2z_R^2} + \frac{(z - z_{\rm sat})^2}{2z_R^2} - \frac{(L_u - z_{\rm sat})^2}{6z_R^2}\right], \qquad (9)$$

and

$$w_{\beta=1}^2(z, L_u) = w_0^2 \left[1 + \frac{2(z - L_u)^2}{3z_R^2} + \frac{(z - z_{\rm sat})^2}{3z_R^2} - \frac{(L_u - z_{\rm sat})^2}{6z_R^2}\right]. \qquad (10)$$

Notice that the spot size is a function of both the observation point (z) and the undulator length (L_u). If on the other hand, the observation point is inside the undulator, *i.e.*, $z < L_u$, we can simply replace L_u by z in Eqs. (9) and (10), then the first term vanishes. The expression of $\beta = 1$ is used as the expected value for the "line source" curve in Fig. 3.

ISBN 978-3-95450-133-5

Based on the line source model, we can compute the effective source location:

$$w_{\text{line}}{}^2(z, L_u) = w_0{}^2\left[1 + \left(\frac{z - z_{\text{eff}}}{z_R}\right)^2\right], \qquad (11)$$

where $w_{\text{line}}{}^2(z, L_u)$ is given in Eq. (7). The effective source location can be obtained by solving the above equation, $z_{\text{eff}}(z) = z - z_R\sqrt{w_{\text{line}}{}^2(z, L_u)/w_0{}^2 - 1}$.

For $\beta = 0$ and $\beta = 1$, the expression for z_{eff} can be simplified by proper approximations to get:

$$z_{\text{eff};\beta=0}(z) \approx \frac{(L_u + z_{\text{sat}})}{2} - \frac{(L_u - z_{\text{sat}})^2}{24z} - \frac{(L_u - z_{\text{sat}})^2(L_u + z_{\text{sat}})}{48z^2}, \qquad (12)$$

and

$$z_{\text{eff};\beta=1}(z) \approx \frac{(2L_u + z_{\text{sat}})}{3} - \frac{(L_u - z_{\text{sat}})^2}{36z} - \frac{(L_u - z_{\text{sat}})^2(2L_u + z_{\text{sat}})}{108z^2}. \qquad (13)$$

The above described model and expressions (for $\beta = 1$) will be compared to the numerical results below.

DECOMPOSING RESULT AND OPTIC PROPERTIES

A tapered undulator scheme is studied to achieve TW power level. Three different types of electron transverse distributions are considered in the study. The electric fields at several different observation points along the undulator are simulated with GENESIS. The electric fields are decomposed by the approach introduced in third section. The decomposition is applied to all three cases with different kind of transverse electron distributions. As shown in Fig. 1, for the Gaussian case, the tapered FEL saturates at about 150 m, hence in the following, we should results up to 150 m. The evolution of the portion of power in the fundamental mode can be clearly obtained after the mode decomposition. Before reporting the results, some related optic properties and FEL characteristics are discussed as in the follows.

The spot size can be calculated by Eq. (3), and the evolution of spot size is shown in Fig. 3. The simulation results are compared to the expected value ("line source") which is introduced above in above section. The expected spot size values of the FEL light are modeled by two physical considerations: one is the gain guiding effect in the exponential growth region, which gives a result that the spot size does not change before the exponential saturation point as the FEL develops along undulator; the other one is that the light emitted from the post saturation region is described by the extended line source model above.

The spot size from the decomposition calculation shows the gain guiding characteristic in all three cases of transverse distributions. The gain guiding effect is fully established at around 20m as in Fig.3. Before 20m, there are modes not satisfying the azimuthal symmetry. Besides, the fundamental mode is not dominating yet before 20m.

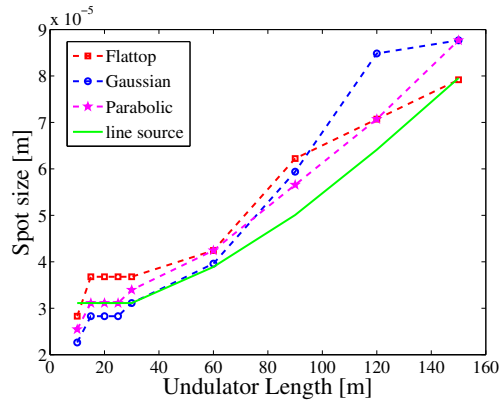

Figure 3: FEL beam spot size varies along the undulator distance.

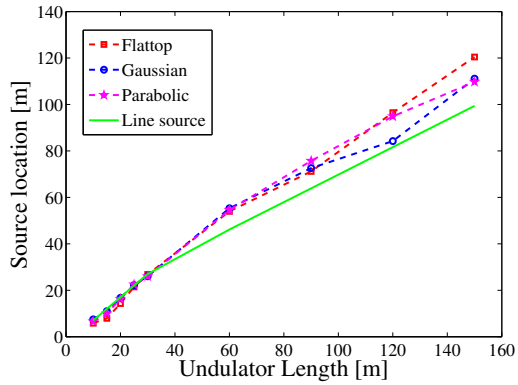

Figure 4: FEL source location varies along the undulator distance.

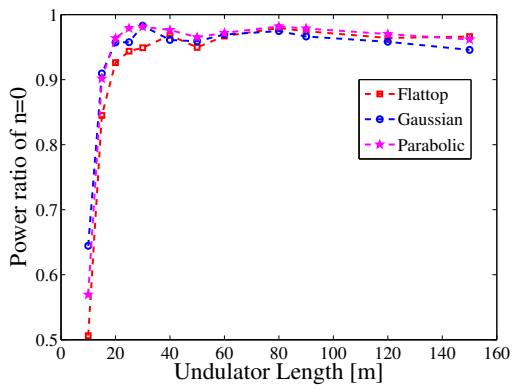

Figure 5: The portion of the fundamental mode power varies along the undulator distance.

The effective beam waist locations, also called the source locations, of all three cases are plotted in Fig. 4 and the expected value is shown together. The expected value is

ISBN 978-3-95450-133-5

defined by two rules. First, in the exponential growth region, the source location is at about one gain length before the observation point. For example: the electric field at 30m has a source location at 27.3m since the gain length here is 2.7m. Second, the extended "line source" model with $\beta = 1$ is adopted to get the effective source location.

For the numerical part, analogy to a laser beam, the FEL effective beam waist location z_s can be evaluated by the wave front curvature $R(z)$ and the spot size $w(z)$ at certain location z. Since we expand the electric field in the Laguerre-Gaussian basis as in Eq. (1), we can write the $R(z)$ and $w(z)$ with $\Re(\zeta)$ and $\Im(\zeta)$:

$$z_s = \frac{R(z)}{1 + \left[\frac{\lambda R(z)}{\pi w(z)^2}\right]^2} = \frac{2\pi}{\lambda}\frac{\Im(\zeta)}{\Im^2(\zeta) + \Re^2(\zeta)} \qquad (14)$$

The results show that in the exponential growth region, the source location is very close to one gain length before the observation point, just as expected. In the post saturation region, the source location is very close to the expected values as in Fig. 4.

The discussion on the spot size and source location evolution reveals some expected FEL properties, which supports that the approach of mode decomposition is reliable. Next, we show how the power of the fundamental mode evolves along the undulator as in Fig. 5. In the plot, in the exponential growth region, the portion of the fundamental mode grows very fast and exceeds 95% at saturation point. In the post saturation region, after 80m, the ratio drops down slightly. However, it is still higher than 90%. This is a very important result. This means that when the TW FEL is achieved by utilizing taper undulator associated with various types of beam transverse distributions, the power portion in the fundamental mode remains high. This ensures that such an FEL light has high transverse coherence.

SUMMARY

The taper undulator scheme with three kinds of transverse electric beam distributions is investigated for a TW FEL. The transverse coherence property is discussed by mode decomposition. An approach of finding the mode contents of a complex electric field generated from GENESIS simulation is proposed and proven to be reliable. It is discovered that in the post saturation region, over 90% of the total power belongs to the fundamental mode. For the three different transverse distributions, the percentage of the fundamental mode power is higher in the flattop and parabolic cases than in the Gaussian case. The high percentage of the fundamental mode guarantees a high transverse coherence. With the knowledge of the mode contents, the source location is also calculated, which provides information for downstream x-ray beam line design.

ACKNOWLEDGEMENT

The authors would like to thank Professor S.-Y. Lee of Indiana University for many stimulated discussions. K.F. would like to express his gratitude to Prof. Lee for many advices. The work was supported by the US Department of Energy (DOE) under contract DE-AC02-76SF00515 and the US DOE Office of Science Early Career Research Program grant FWP-2013-SLAC-100164. The work of K.F. was also supported by the US DOE grant DE-FG02-12ER41800 and National Science Foundation grant NSFPHY-1205431.

REFERENCES

[1] H.N. Chapman, P. Fromme, A. Barty, T.A White, R.A. Kirian, A. Aquila, M.S. Hunter, J. Schulz, D.P. DePonte, U. Weierstall, R.B. Doak, F.R.N.C. Maia, A. Martin, I. Schlichting, "Femtosecond X-ray protein nanocrystallography", Nature **470**, 73-78 (2011).

[2] M.M. Seibert, T. Ekeberg, F.R.N.C. Maia, M. Svenda, J. Andreasson, O. Jönsson, D. Odić, B. Iwan, A. Rocker, D. Westphal, M. Hantke, D.P. DePonte, "Single mimivirus particles intercepted and imaged with an X-ray laser", Nature **470**, 78-81 (2011).

[3] N.M. Kroll, P.L. Morton, M.R. Rosenbluth, "Free-Electron Lasers with Variable Parameter Wigglers", IEEE J. Quantum Electron., **QE-17**, 1436-1468 (1981).

[4] X. Wang, H. Freund, D. Harder, W. Miner, J. Murphy, H. Qian, Y. Shen, and X. Yang, "Efficiency and Spectrum Enhancement in a Tapered Free-Electron Laser Amplifier", Phys. Rev. Lett. **103**, 154801 (2009).

[5] Y. Jiao, J. Wu, Y. Cai, A.W. Chao, W.M. Fawley, J. Frisch, Z. Huang, H.-D. Nuhn, C. Pellegrini, S. Reiche, "Modeling and multidimensional optimization of a tapered free electron laser", Phys. Rev. ST Accel. Beams, **15**, 050704 (2012).

[6] F. Gori, M. Santarsiero, R. Simon, G. Piquero, R. Borghi, and G. Guattari, "Coherent-mode decomposition of partially polarized, partially coherent sources", Journal of the Optical Society of America A, **20**, 78-84 (2003).

[7] S. Reiche, "GENESIS 1.3: a fully 3D time-dependent FEL simulation code", Nucl. Instrum. Methods A, **429**, 243 (1999).

[8] J. Wu and L.H. Yu, "Eigenmodes and mode competition in a high-gain free-electron laser including alternating-gradient focusing", Nucl. Instrum. Methods A, **475**, 79-85 (2001).

ISBN 978-3-95450-133-5